1996

Development of a Biologically Based Aerobic Composting Simulation Model

Dennis P. Stombaugh
The Ohio State University

Sue E. Nokes
University of Kentucky, sue.nokes@uky.edu

Development of a Biologically Based Aerobic Composting Simulation Model

Digital Object Identifier (DOI)
https://doi.org/10.13031/2013.27504

Notes/Citation Information
Published in *Transactions of the ASAE*, v. 39, issue 1, p. 239-250.

DEVELOPMENT OF A BIOLOGICALLY BASED AEROBIC COMPOSTING SIMULATION MODEL

D. P. Stombaugh, S. E. Nokes

ABSTRACT. *A relatively simple dynamic model based on microbial process kinetics has been developed for aerobic composting. Differential equations describing microbial, substrate, and oxygen concentrations, as well as moisture and temperature profiles have been derived as a function of vessel size and aeration rate. Microbial biomass growth was described using Monod growth kinetics as a function of degradable substrate concentration, oxygen concentration, moisture content, and compost temperature. Facility and fan operating costs have been included to permit economic optimization of the process. Predicted results demonstrated the ability of the model to quantify and describe the influence of multiple interacting factors (temperature, oxygen, moisture, and substrate availability) on the process driving the composting: microbial growth kinetics. Future development of the approach should be undertaken to provide a robust engineering model that can be used to evaluate and design environmentally sound composting facilities. An example application is presented along with data from a laboratory scale composter.* ***Keywords.*** *Aerobic composting, Bioreactor systems, Biological engineering, Dynamic modeling, Engineering education.*

Process models describing aerobic composting have been developed and used effectively in design (Haug, 1986a, b, c; Haug and Tortorici, 1986; Keener et al., 1991, 1993a, b; Person and Shayya, 1994; Hogan et al., 1989), however, the underlying biological portion of the process has been largely neglected. Hamelers (1993) made a significant contribution by including the biological component in a model which examined the kinetics of composting at the particle level. The model effectively calculated gradients of oxygen, biomass, and soluble and polymeric substrate in the boundary layer surrounding individual particles. A model is needed for engineering design which includes process parameters based on fundamental microbial kinetics. A kinetic model would be more robust than current empirical models and would provide more complete insights into the complexities of the composting process.

The primary objective of this project was to develop a composting model based on Monod kinetics which could be used for engineering analysis and design. The model describes microbial growth and compost degradation as a function of substrate and oxygen concentration, temperature, moisture content, depth of compost, and air flow rate. Realistic cost constraints were included to evaluate and optimize an in-vessel composting process using a lumped parameter dynamic simulation. The second objective of this work was to demonstrate the usefulness of the model with an example application.

Article was submitted for publication in February 1995; reviewed and approved for publication by the Emerging Areas Div. of ASAE in September 1995. Presented as ASAE Paper No. 94-3616.

Salaries and research support provided by state and federal funds appropriated to the Ohio Agricultural Research and Development Center, The Ohio State University, Columbus, Ohio. Approved as Journal No. 66-95.

The authors are **Dennis P. Stombaugh** ***ASAE Member Engineer,*** Professor Emeritus, Dept. of Agricultural Engineering, The Ohio State University, Columbus, Ohio; and **Sue E. Nokes,** ***ASAE Member Engineer,*** Assistant Professor, Dept. of Biosystems and Agricultural Engineering, University of Kentucky, Lexington. **Corresponding author:** Sue E. Nokes, Dept., of Biosystems and Agricultural Engineering, University of Kentucky, Lexington, KY 40546; e-mail: <snokes@bae.uky.edu>.

MODEL DEVELOPMENT

The growth rate of the microbes in each of n layers of compost [dX/dt, $kg_{cells}/(m^3 \cdot h)$] can be written as:

$$\left(\frac{dX}{dt}\right)_{j,t} = (\mu)_{j,t-1} \times X_{j,t-1} - k_d \times (X)_{j,t-1} \qquad (1)$$

where

- j = layer within compost (j = 1 to n)
- μ = specific growth rate (h^{-1})
- k_d = specific death rate (h^{-1})
- t = time (h)

In this model, X represents total microbial biomass concentration including mesophilic and thermophilic bacteria, actinomycetes, and fungi.

The substrate, S, was assumed to be the readily degradable fraction of the dry matter available for composting. The rate of substrate consumption (dS/dt, $kg/h \cdot m^3$) was assumed to be:

$$\left(\frac{dS}{dt}\right)_{j,t} = \frac{1}{Y_{X/S}} \times \left(\frac{dX}{dt}\right)_{j,t} + (\beta)_{j,t-1} \times (X)_{j,t} \qquad (2)$$

where

- $Y_{X/S}$ = yield coefficient, kg cells produced/kg substrate consumed
- β = microbial maintenance coefficient, $kg_S/(kg_X \cdot h)$

The following expressions were developed to include the effects of oxygen concentration, substrate availability, temperature, and moisture, assuming multiplicative or

interactive Monod relationships for μ (the specific growth rate) as well as β (the microbial maintenance coefficient):

$$(\mu)_{j,t} = \mu_{max} \times \frac{(S)_{j,t}}{K_s + (S)_{j,t}} \times \frac{(O_2)_{j,t}}{K_{O_2} + (O_2)_{j,t}} \times (ktemp)_{j,t} \times (kH_2O)_{j,t} \quad (3)$$

$$(\beta)_{j,t} = \beta_{max} \times \frac{(S)_{j,t}}{K_s + (S)_{j,t}} \times \frac{(O_2)_{j,t}}{K_{O_2} + (O_2)_{j,t}} \times (ktemp)_{j,t} \times (kH_2O)_{j,t} \quad (4)$$

where

μ_{max} = maximum specific growth rate (h^{-1})
β_{max} = maximum microbial maintenance coefficient ($kg_S/(kg_x \cdot h)$
K_S = half velocity constant for degradable substrate (kg_S/m^3)
K_{O_2} = half velocity constant for oxygen (kg_{O_2}/m^3)
$(ktemp)_{j,t}$ = temperature (T, °C) coefficient for all microorganisms

$= T/(T_2 - T_1)$ $\quad T_1 < T \le T_2$
$= 1.0$ $\quad T_2 < T \le T_3$
$= 3.75 - [T/(T_2 - 10)]$ $\quad T_3 < T$ (5)

$(kH_2O)_{j,t}$ = moisture (m, kg/kg wet basis) coefficient

$= 0.0$ $\quad m_1 < m \le m_2$
$= (m/m_2) - 1.0$ $\quad m_2 < m \le m_3$
$= 1.0$ $\quad m_3 < m$ (6)

T_1, T_2, T_3, m_1, m_2, m_3 = empirically set constants

Although more complex expressions for ktemp were examined, the final expressions were chosen based on their ability to predict growth rates as a function of temperature and for their simplicity. Since the microbial biomass has several distinct components which respond to temperature differently, the values for ktemp represent a summation of the responses of the individual microbial populations.

The rate of change in the oxygen concentration [dO_2/dt, $kg_{O_2}/(m^3 \cdot h)$] in each of the n layers of compost was derived as:

$$\left(\frac{dO_2}{dt}\right)_{j,t} = Y_{O_2/S} \times \left(\frac{dS}{dt}\right)_{j,t} + F \times \frac{n}{\rho} \times (O_{2\,in\,j,t} - O_{2\,j,t-1}) \quad (7)$$

where

Y_{O_2} = yield coefficient, kg O_2 produced/kg substrate consumed
F = flow rate for entire composter = $kg_{da}/(h \cdot m^3)$
n = number of layers
ρ = specific air density, kg_{da}/m^3
$(O_2)_{j,t-1}$ = oxygen concentration of layer, kg_{O_2}/m^3
$(O_{2in})_{j,t}$ = oxygen concentration of air entering the layer = oxygen concentration of previous node, kg_{O_2}/m^3

The oxygen uptake rate for the entire composter can be calculated by:

$$OUR = \frac{F}{\rho}(O_{2\ inlet} - O_{2\ outlet}) \quad [kg_{O_2}/(h \cdot m^3)] \quad (8)$$

The rate of change in the water content [dW/dt, $kg_{H_2O}/(m^3 \cdot h)$] for each layer was written as:

$$\left(\frac{dW}{dt}\right)_{j,t} = Y_{W/S} \times \left(\frac{dS}{dt}\right)_{j,t} - F \times n \times (w_{in\,j,t} - w_{out\,j,t-1}) \quad (9)$$

where

$Y_{W/S}$ = yield coefficient (kg water produced/kg substrate consumed)
$(w_{in})_{j,t}$ = humidity ratio of air entering layer $[kg_{H_2O}/kg_{da} = (w_{out})_{j-1,t}]$
$(w_{out})_{j,t-1}$ = humidity ratio of air leaving layer, (kg_{H_2O}/kg_{da})
$m_{j,t}$ = moisture content (kg/kg wet basis)

$$m_{j,t} = W_{j,t} / (S_{j,t} + NVS_{j,t} + W_{j,t}) \quad (10)$$

$(NVS)_{j,t}$ = nonvolatile solids (kg/m^3)
$(W)_{j,t}$ = mass of water (kg/m^3)

Based on the rate of change in energy in each layer, the following equation for temperature (T, °C) was derived:

$$\left(\frac{dT}{dt}\right)_{j,t} = \left\{-Y_{H/S} \times \left(\frac{dS}{dt}\right)_{j,t} - F \times n \times [h_{i(j,t)} - h_{o(j,t-1)}] - cond\right\} / (T_{mass})_{j,t} \quad (11)$$

where

$Y_{H/S}$ = yield coefficient (joule of heat produced/kg substrate consumed)
cond = horizontal loss of heat through the composter wall $[J/(h \cdot m^3)]$
$(T_{mass})_{j,t-1}$ = thermal mass of layer $[J/(°C \cdot m^3)]$

$$(T_{mass})_{j,t} = C_w \times W_{j,t} + C_{NVS} \times (NVS)_{j,t} + C_s \times (S)_{j,t} \quad (12)$$

where

C_W = specific heat of W = 4180 J/(kg·°C)
C_{NVS} = specific heat of NVS = J/(kg·°C)
C_S = specific heat of S = J/(kg·°C)
$(h_i)_{j,t}$ = enthalpy of inlet air to node (J/kg_{da})
$(h_o)_{j,t-1}$ = enthalpy of outlet air from node (J/kg_{da})

A psychrometric subroutine was included in the model to calculate enthalpies and humidity ratios based on dry bulb and dew point temperatures. It was assumed that the air leaving a layer was at the dry bulb temperature of the layer and that the air was saturated at that temperature if the moisture content of the layer was greater than 18%. If the moisture content of the layer was less than or equal to

18%, the dew point temperature of the air remained unchanged from the previous layer.

To determine power requirements, the pressure drop (ΔP, mm H_2O) through the compost material was estimated by the following equation adapted from Higgins et al. (1982):

$$\Delta P = a \times (vel)^{1.48} \times d^{1.41} \quad (13)$$

where

vel = flow velocity (m/min)
d = depth (m)
a = empirical coefficient

Fan power requirements (P_W; Watts) were calculated from:

$$P_W = \frac{Q \times \Delta P}{367.3 \times eff} \quad (14)$$

where

Q = air flow delivery (m^3/h)
ΔP = pressure drop (mm H_2O)
eff = fan efficiency

Given initial investment cost data for compost bin construction versus depth and fan cost versus power requirements, the depth of compost, fan sizes, control strategies for each fan, and the length of each composting cycle can be determined to minimize $/$kg_S$ processed.

Example Application

A mixture of equal weights of cracked corn and pelleted corn cobs at an initial moisture content of 60% (wet basis) was used as an example composting mixture. For simplicity, the corn (C_{34} H_{64} 0_{24} N_1) in the composting mixture was assumed to be the primary ingredient to degrade, due to its nearly optimal C/N ratio of 29.1 (Keener et al., 1993b):

$$C_{34}H_{64}O_{24}N_1 + 37.25\ O_2 \rightarrow 34\ CO_2 + 30.5\ H_2O + NH_3 \quad (15)$$

Parameter Estimation

Using equation 15 and knowing the molecular weights of each compound, 870 g of substrate reacts with 1 192 g of oxygen to produce 1 496 g of carbon dioxide, 549 g of water, and 17 g of ammonia. From this information and the heat of combustion of corn (19.1×10^6 J/kg), the following yield coefficients were determined for each kilogram of substrate:

$$Y_{O_2/S} = 1.370 \quad (kg_{O_2}/kg_S)$$

$$Y_{H/S} = 19.1 \times 10^6 \quad (J/kg_S)$$

$$Y_{CO_2/S} = 1.720 \quad (kg_{CO_2}/kg_S)$$

$$Y_{W/S} = 0.631 \quad (kg_{H_2O}/kg_S)$$

For the mixture of corn and corn cobs used in this example, the degradable fraction was assumed to be the volatile solids content. Keener et al. (1993b) presents a discussion related to the difficulty of defining and measuring "readily degradable". A value of 87% of the corn and corn cob mixture was assumed to be the degradable fraction (Keener et al., 1993b).

Coefficient and parameter values were estimated from experimental data and the literature (Haug, 1980). For example, μ_{max} was estimated from laboratory composter experiments assuming logarithmic growth. Assumed values for X and measured oxygen uptake rates during the stationary phase were used to estimate β_{max}. Estimates for K_{O_2}, K_S, $Y_{X/S}$, and $X_{initial}$ were obtained by examining other composting data (Haug, 1980; Elwell et al., 1994; Hansen et al., 1993). A list of the coefficient and parameter values used in the example simulation for default values is shown in table 1. The simulation model was programmed for the case of n layers using rectangular integration with an integration interval of 0.01 h.

To demonstrate the usefulness of the model for design, a composting facility similar to a batch grain drying system with stirring devices and two fans was specified. Initially the air flow rate [F; $kg_{da}/(h \cdot m^3)$] was either fixed at 10.0 or controlled by the air outlet temperature (T; °C) as follows:

F = 2.5	T < 55
F = 25.0	T ≥ 58
Unchanged	55 < T < 58

The following data were estimated from commercial literature and a building cost guide (Boeckh, 1994) for an 11 m diameter, modified grain bin, having one small fan and one large fan. It was assumed that the total annual facilities cost was 25% of the initial investment. Twenty-four hours were allotted for loading and unloading each batch.

Bin, stirring devices, and one small fan	= 15,500 + 3,300 × d ($)
d	= depth of compost (m)
Large fan cost	= 1.500 + 0.150 × P_W ($)
P_w	= large fan size (Watt)
Fan operating costs	= 0.08 ($/kW·h)
Material handling and preparation	= 1.00 ($/$m^3$)

Table 1. Coefficient and parameter values used in example application

Parameter		Default
μ_{max}	h^{-1}	0.200
k_d	h^{-1}	0.0250
β_{max}	$kg_S/(kg_X \cdot h)$	0.480
$Y_{X/S}$	kg_X/kg_S	0.3500
K_s	kg/m^3	62.0
K_{O_2}	kg/m^3	0.070
X_{init}	kg/m^3	0.008
T_1	°C	0
T_2	°C	30
T_3	°C	55
m_1	(kg/kg w.b.)	0
m_2	(kg/kg w.b.)	0.2
m_3	(kg/kg w.b.)	0.4
a	(dimensionless)	28.6
eff	(dimensionless)	0.4
C_{NVS}	J/(kg·°C)	840
C_S	J/(kg·°C)	1480
F	$kg_{da}/(h \cdot m^3)$	10.0

Laboratory Composter

A laboratory composter was constructed from cylindrical PVC tubing with an inside diameter of 0.305 m and a maximum compost depth of 0.91 m. Commercially available end caps were used. A 0.10 m air space was provided between the compost and the end caps at both ends of the cylinder. Air flow was monitored with a TSI, Inc. model 2013D mass flowmeter, which was computer controlled at a nominal dry air (da) delivery of 1.0 kg_{da}/h using a variable speed 12 V d.c. fan. Using four inlet and outlet valves, it was possible to reverse the direction of airflow.

Data collected included inlet (room) temperature, compost temperature at five levels, air flow rate, and outlet oxygen (Beckman, model F3M3) and carbon dioxide (Mine Safety Appliances, model 303) levels. Temperatures were measured using type T thermocouple probes. Data were taken at 30 s intervals and averaged to obtain hourly data which were permanently recorded for analysis following the 10-day composting trial.

A mixture of cracked corn (9-kg dry matter) and pelleted corn cobs (9-kg dry matter) adjusted to a 60% initial moisture content (wet basis) was used. The air flow direction was from top to bottom to facilitate collection of condensed water vapor. The compost mixture was left overnight in a covered container with no air flow for approximately 20 to 24 h prior to placement into the composting vessel.

Results

Five scenarios were investigated with the simulation model. The first simulations investigated the interactions between microbial biomass growth, oxygen concentration, temperature, substrate concentration, and moisture content for five layers within the composter using a constant aeration rate. Next, the effect of different constant aeration rates on performance of a single layer of compost was evaluated. In the third set of simulations using a five-layer composter set-up, the aeration rate was controlled by the exhaust air temperature. The fourth set of simulations investigated the cost of composting versus the depth of compost. The last group of simulations consisted of sensitivity analyses which determined the effects of varying key parameters.

Figures 1a through 1f illustrate the ability of the model to predict patterns of biomass growth and substrate use and the interactions with temperatures, oxygen concentrations, and moisture levels at different positions within the vessel. These variables are shown for all five layers for a constant flow rate of 10 $kg_{da} \cdot h^{-1} \cdot m^{-3}$.

Initially, predicted biomass growth in the first two layers was delayed (fig. 1a) due to evaporative cooling in these layers (fig. 1d). The growth rates in each of the first layers and the transport of heat into each following layer caused the final layers to rapidly reach high temperatures. The magnitudes of the incremental increases in temperature between layers reflected the biomass growth and substrate degradation rates occurring within each layer both theoretically (figs. 1a, 1b, and 1d) and experimentally (fig. 7b). Temperatures higher than 55°C (fig. 1d) and the slightly reduced oxygen concentrations (fig. 1e) inhibited biomass growth rates in the last three layers (fig. 1a) beginning 60 to 70 h into the simulated run. The resulting growth patterns caused biomass concentrations to peak sequentially from the first to the last layers (fig. 1a). The biomass concentrations then declined rapidly and sequentially (fig. 1a). The rapid decrease in biomass concentrations and rates of substrate consumption (fig. 1b) was the result of sequential reductions in moisture content in each layer (fig. 1f). Corresponding decreases and oscillations were observed in the layer temperatures (fig. 1d) and oxygen concentrations (fig. 1e). Corresponding substrate concentrations are shown in figure 1c.

Figures 2a through 2f illustrate predicted rates of composting versus time as a function of airflow rate assuming only one layer (perfect mixing). Flow rates of 1, 5, 10, 15, and 20 $kg_{da}h^{-1}m^{-3}$ were examined. Simulations using one layer provided results similar to simulations using five layers in terms of relative rates of composting and shifting patterns with respect to time as a function of flow rate; however, predicted responses using one layer were not equal to the average value of the predicted results using five layers. Compare the results for one layer with a flow rate of 10 $kg_{da}/(h \cdot m^3)$ to figures 1a through 1f with five layers at the same aeration rate. Using five layers the overall average reduction in substrate was 33.5% compared to a predicted reduction of 39.1% with one layer (fig. 2c). Maximum rates of composting were predicted to occur slightly earlier with five layers as compared to one. Predictions using one node also tended to be much smoother and the small oscillations in temperature and oxygen levels for five layers (figs. 1d through 1e) did not appear in the one layer model. The pronounced shift in maximum composting parameters to earlier times with higher flow rates (figs. 2a through 2b) were also observed in simulations using five layers (data not shown).

The delayed rate of composting predicted (figs. 2a and 2b) at the lowest flow rate (1.0 $kg_{da} \cdot h^{-1} \cdot m^{-3}$) was caused by the low oxygen concentration (fig. 2e) and eventually the temperature which was slightly above optimal (fig. 2d). At this low flow rate the moisture level actually increased slightly (fig. 2f) due to the moisture produced during substrate breakdown which exceeded the moisture removal at the low airflow rate. At the next lowest aeration rate (5.0 $kg_{da} \cdot h^{-1} \cdot m^{-3}$) the low oxygen concentration reduced substrate degradation slightly, but the primary factor reducing biomass growth was the rapid development of the high temperatures (fig. 2d). The oscillations in substrate degradation (fig. 2b) and oxygen levels (fig. 2e) occurring between 65 and 75 h were caused by the small decreases in specific growth rate for temperatures above 55°C. At high aeration rates biomass growth and substrate consumption reached higher maximum values sooner due to more optimal oxygen and temperature levels; however, the higher flow rates also caused more rapid drying and the peak values decreased very rapidly due to low moisture levels (fig. 2f). The self limiting nature of the resulting temperatures was illustrated in figure 2d with maximum temperatures between 67 and 70°C for all flow rates between 5 and 25 $kg_{da} \cdot h^{-1} \cdot m^{-3}$. Total loss of substrate was highest with the intermediate flow rate of 10 $kg_{da} \cdot h^{-1} \cdot m^{-3}$ (fig. 2c).

A simple control strategy to regulate the aeration rate at 2.5 $kg_{da} \cdot h^{-1} \cdot m^{-3}$ when temperature was below 55°C and at

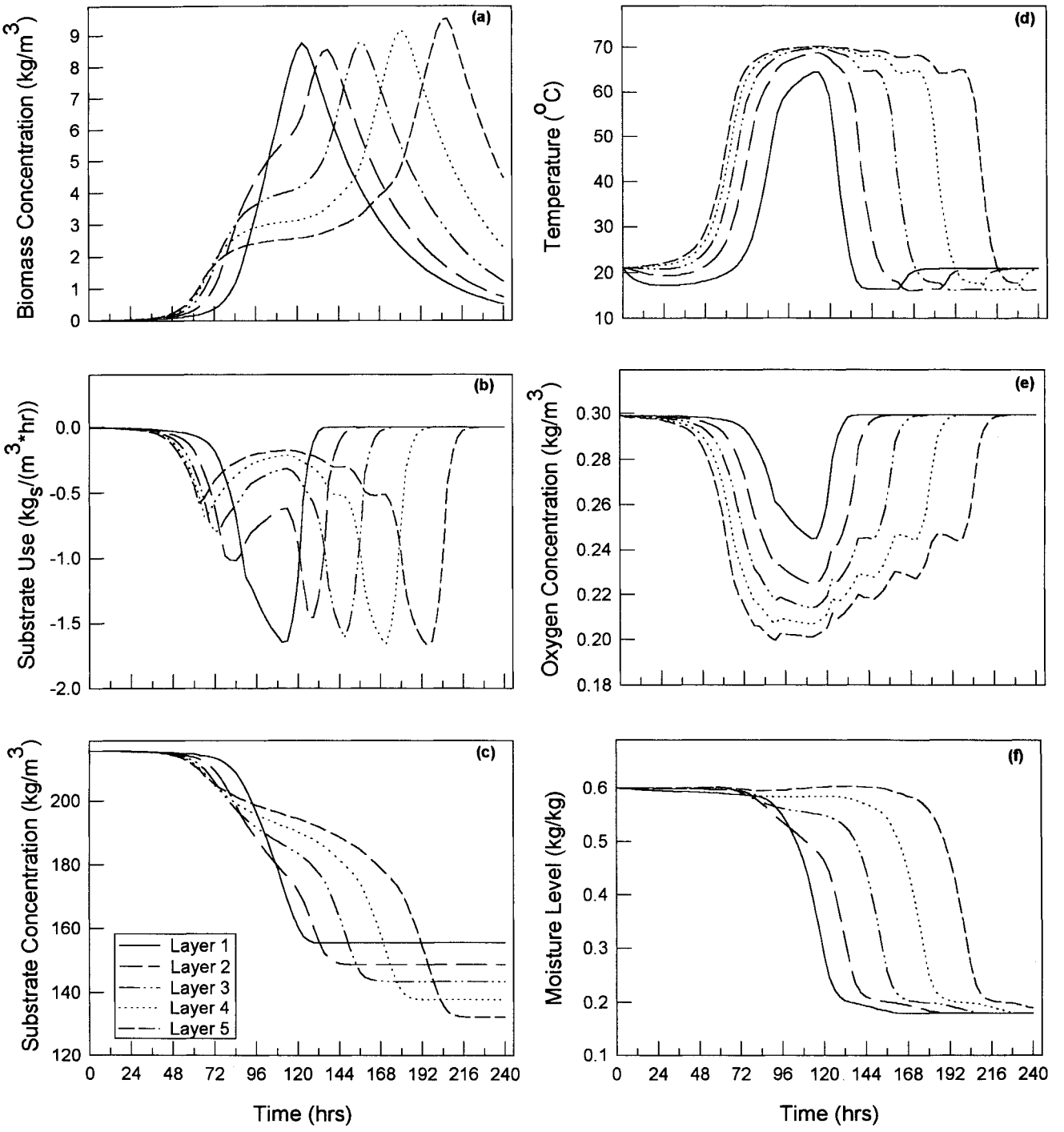

Figure 1–Predicted composter performance vs. time for a constant aeration rate of 10 $kg_{da}/(m^3 \cdot h)$ using a five-layer analysis. Air enters at layer 1 (top) and is exhausted from layer 5 (bottom).

25.0 $kg_{da} \cdot h^{-1} \cdot m^{-3}$ when the temperature was greater than 58°C was incorporated into the program. A 3°C deadband in which no change in flow rate occurred was provided between 55 and 58°C. Results from simulations using this control strategy are shown in figures 3a through 3f. During the initial lag phase, oxygen concentration (fig. 3e) became the limiting factor between 48 and 60 h. The low initial flow rate did promote rapid increases in temperature (fig. 3d) and prevented significant moisture loss (fig. 3f). As the large fan was turned on (crosshatched region, fig. 3e) at approximately 60 h, oxygen concentrations increased rapidly, and substrate degradation rates sequentially reached extremely high levels (2.5-3.0 $kg \cdot h^{-1} \cdot m^{-3}$) within individual layers and rapid moisture losses (fig. 3f) were observed. High aeration and the accompanying evaporative cooling resulted in temperature decreases below inlet air temperature following the end of the rapid composting phase in each of the first three layers.

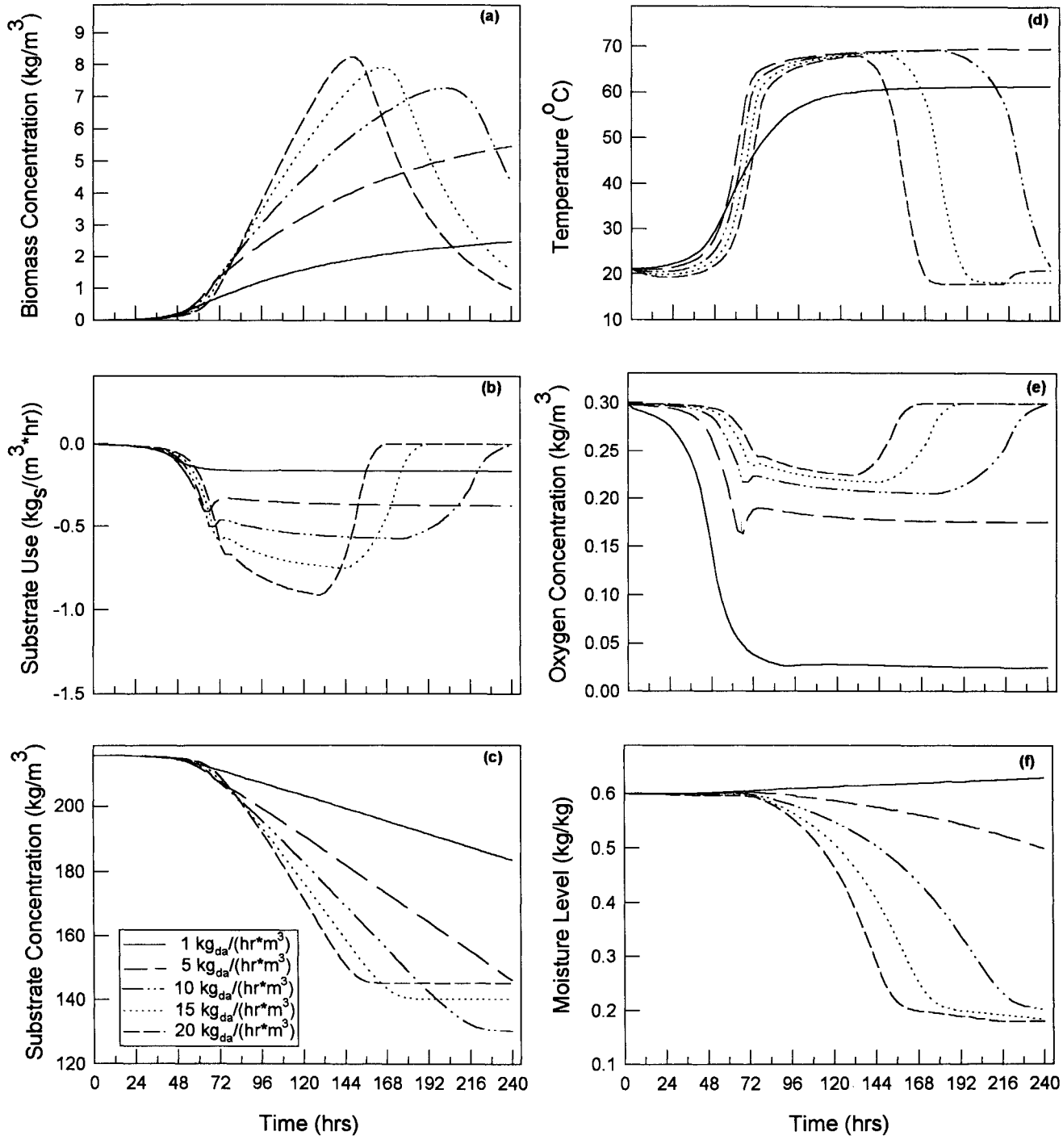

Figure 2–Predicted composter performance vs. time for selected, constant aeration rates using a one-layer analysis.

The model was used to economically optimize the compost depth ($/m^3) for an assumed 15-day processing time and the given fan sizes. The optimal depth was approximately 3.4 m with a total predicted cost of $2.31/m^3 of compost processed (fig. 4). At small depths, the facility cost/m^3 of compost was very high. Facility cost decreased as depth increased to 5 m. At greater depths, facility costs started to increase due to the extremely large fan size required. As expected, fan operating costs ($/m^3) increased dramatically as depth increased. Given the option to reduce the length of the processing cycle or specify alternative fan sizes and control strategies the predicted total costs could be reduced to $1.61/m^3 of compost processed with a cost of $0.028/kg of substrate degraded. This was achieved by changing the larger fan size to approximately 15 $kg_{da} \cdot h^{-1} \cdot m^{-3}$ and reducing the processing time to seven days.

A simple sensitivity analysis was performed to evaluate the relative importance of selected model parameters. The parameter values examined were maximum specific growth rate μ_{max}, specific death rate (k_d), maximum maintenance coefficient (β_{max}), yield coefficient ($Y_{X/S}$), half velocity

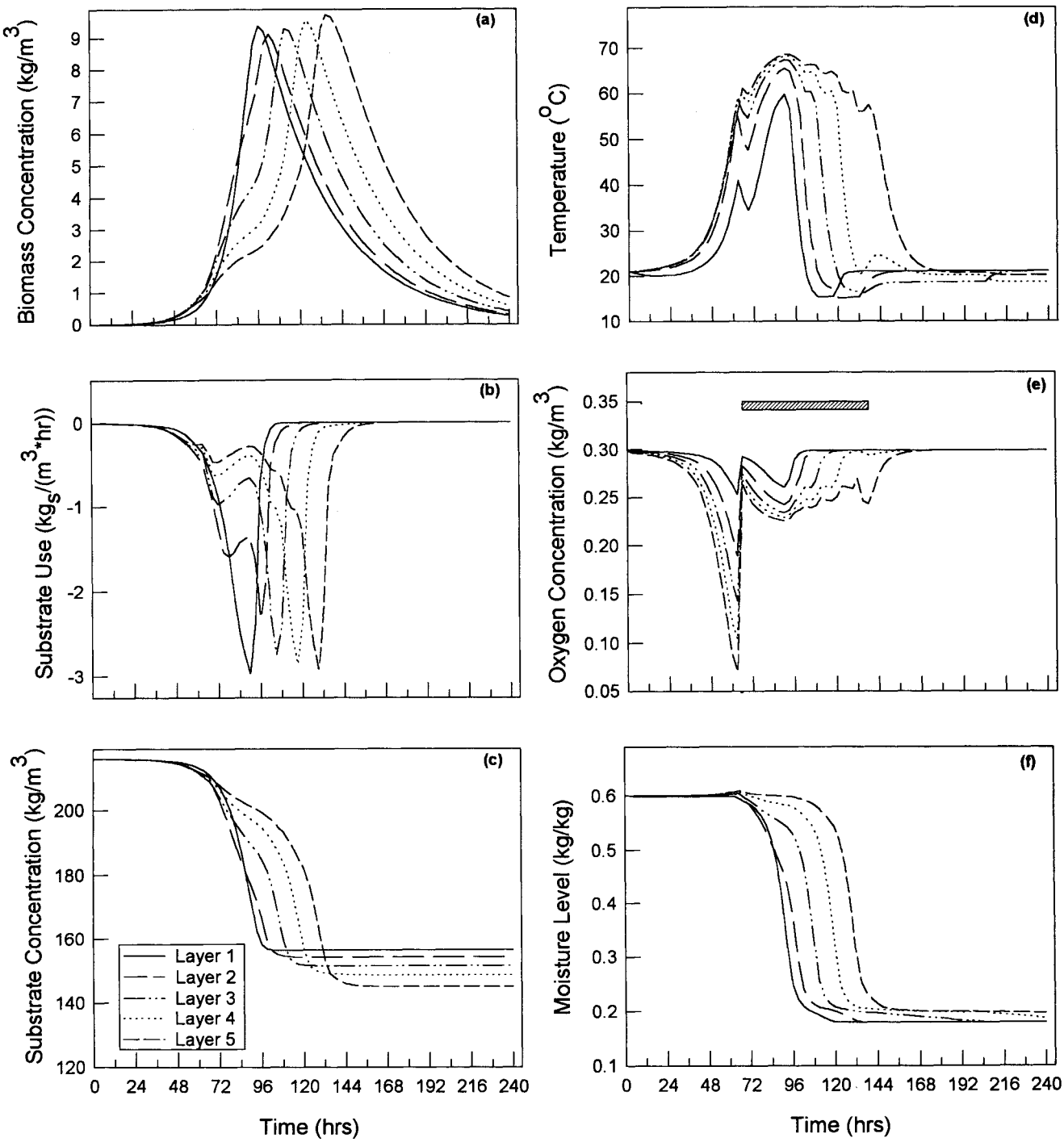

Figure 3–Predicted composter performance vs. time using a five-layer analysis with aeration rate controlled by exhaust air temperature. Aeration rate was 25 $kg_{da}/(m^3 \cdot h)$ during the time period shown by crosshatching in (e). At other times the aeration rate was 2.5 $kg_{da}/(m^3 \cdot h)$.

constants for both degradable substrate (K_S) and oxygen (K_{O_2}), initial biomass concentration (X_{init}), and aeration rate (F). These parameters were varied individually in a one-layer simulation run. The dimensions of the laboratory composter were used and all other parameters were set at their default values. Then each parameter was decreased to both 50 and 25% of its default value and then increased by both 50 and 100% of its default value over a 10-day simulation period. As each parameter was varied, all other parameters were maintained at their default values. All

Table 2. Parameter values used in sensitivity analysis

Parameter		Percentage Change in Parameter Values				
		−50	−25	Default	+50	+100
μ_{max}	h^{-1}	0.100	0.150	0.200	0.300	0.400
k_d	h^{-1}	0.0125	0.0188	0.0250	0.0375	0.0500
β_{max}	$kg_S/(kg_X \cdot h)$	0.240	0.360	0.480	0.720	0.960
$Y_{X/S}$	kg_X/kg_S	0.1750	0.2625	0.3500	0.5250	0.7000
K_s	kg/m^3	31.0	46.5	62.0	93.0	124.0
K_{O_2}	kg/m^3	0.035	0.0525	0.070	0.105	0.140
X_{init}	kg/m^3	0.004	0.006	0.008	0.012	0.016
F	$kg_{da}/(h \cdot m^3)$	5.0	7.5	10.0	15.0	20.0

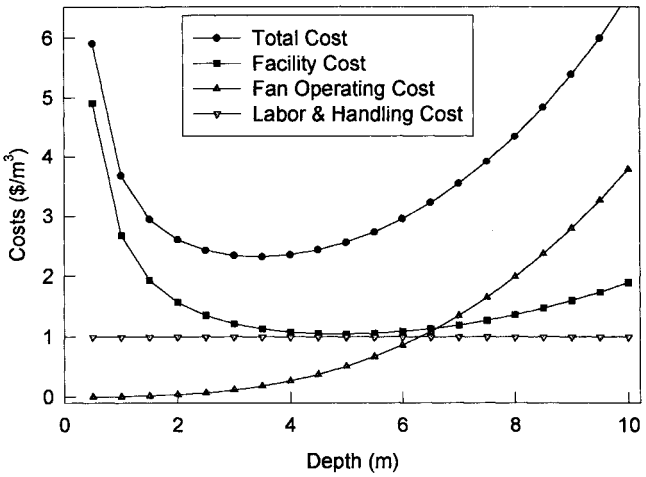

Figure 4–Composting costs as a function of depth for the example aeration control system.

parameter values used are shown in table 2. Results from this analysis are shown graphically in figures 5 and 6.

The output values examined were the maximum biomass concentration at any time (X_{max}, kg/m^3), the total percent reduction in readily degradable volatile solids during the 10-day simulation (ΔS, %), the maximum compost temperature (T_{max}, °C) at any time, and the maximum rate of substrate degradation during the 10-day simulation. In figures 5 and 6 the effects of changes in each parameter value on these four outputs are shown. For example as μ_{max} varied from 0.10 to 0.40 h^{-1}, X_{max} increased from 1.72 to 12.47 kg/m^3 (fig. 5a).

The sensitivity analysis demonstrated that several factors in the process (temperature, oxygen, and moisture) interacted to control the rates of reactions and the

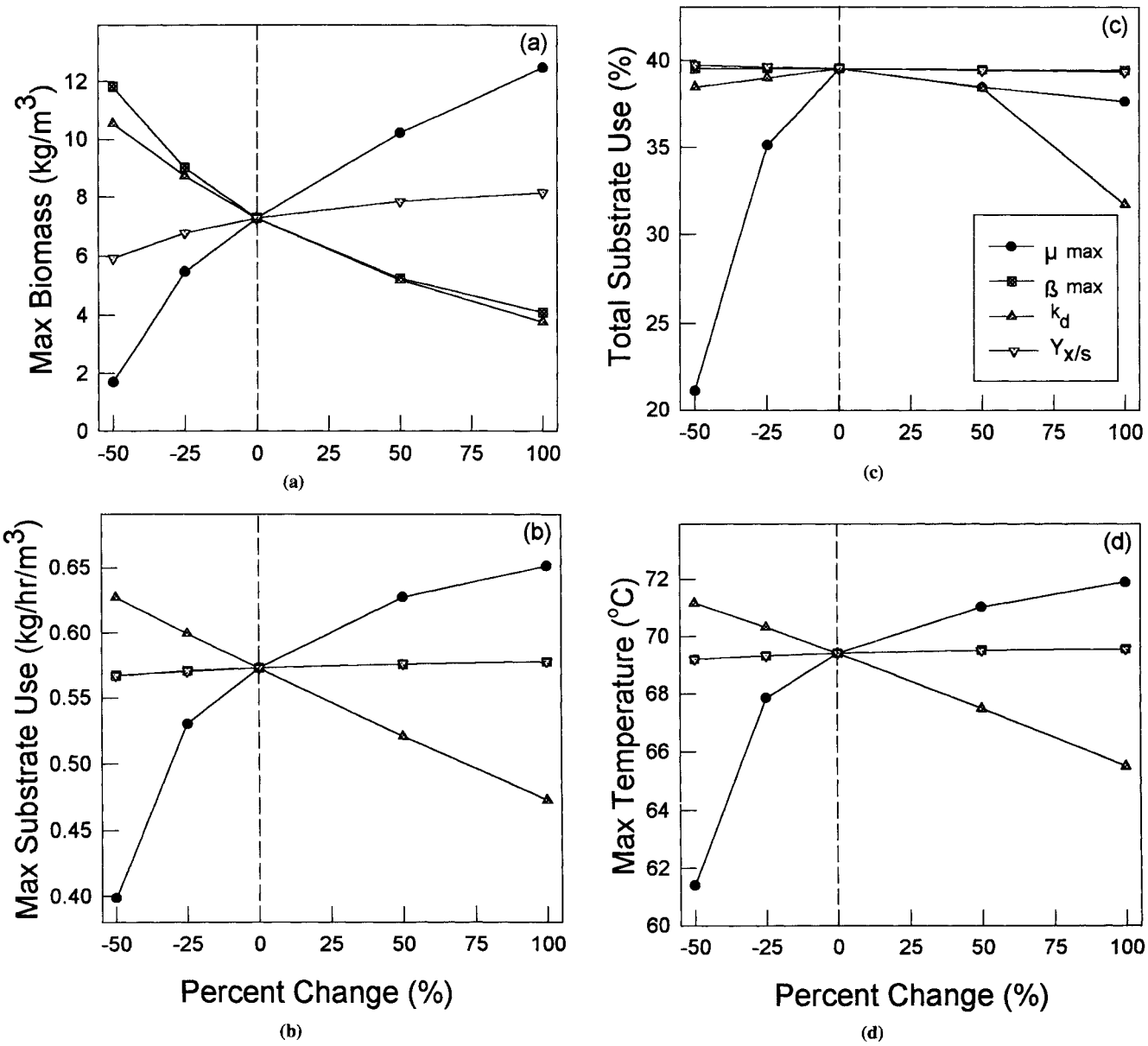

Figure 5–Sensitivity analysis showing predicted model outputs as the indicated parameter (μ_{max}, β_{max}, k_d, or $Y_{X/S}$ altered from –50 to +100% of its default value. (a) Maximum biomass concentration. (b) Maximum rate of substrate utilization. (c) Total percent reduction in substrate concentration during the 10-day simulation period. (d) Maximum temperature.

interpretation of the results was not always straight forward due to these multiple interactions. For example, as μ_{max} increased or as k_d decreased, fairly large increases in X_{max} occurred (fig. 5a). With these increases in X_{max} corresponding increases in T_{max} (fig. 5d) and in dS/dt (fig. 5b) occurred; however, these changes were much less pronounced than the changes in X_{max}. The decreased sensitivity of these outputs was due to limits placed on the growth process by the oxygen concentrations and temperatures. Even more pronounced interactions were observed in the effect of increased μ_{max} or decreased k_d on the total reduction in substrate (fig. 5c). The maximum total substrate degradation (39.5%) occurred at the intermediate default values of μ_{max} = 0.2 h^{-1} and k_d = 0.025 h^{-1}. As μ_{max} increased from its default value by 100%, an increase in X of only 71% occurred because growth was inhibited somewhat by reduced 0_2 levels and higher temperatures. Similarly, an increase in the maximum rate of substrate degradation was observed, but it was increased by only 14%. The slightly higher temperature when μ_{max} was increased by 100% (71.9 vs. 69.4°C) caused more rapid drying. The slightly higher rates of substrate degradation at the increased μ_{max} values were terminated much earlier due to low moisture levels. This shorter duration of the peak rates of composting actually caused the total substrate reduction to decrease from 39.53 to 37.66% even though the maximum substrate degradation rates and biomass concentrations were higher.

Changes in β_{max} or $Y_{X/S}$ had very little effect on the maximum rates of composting (fig. 5b), total substrate reduction (fig. 5c), and maximum compost temperatures

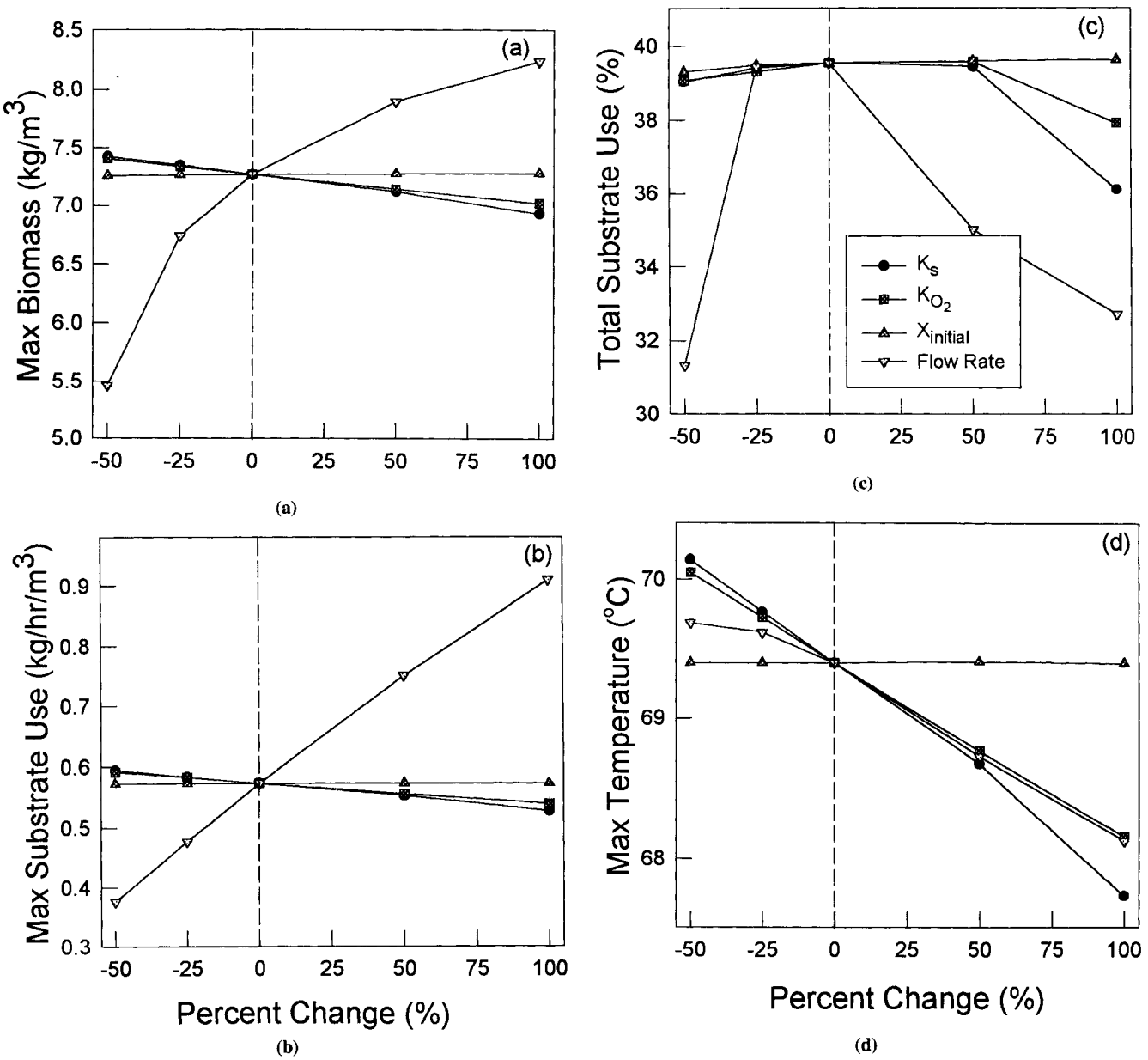

Figure 6–Sensitivity analysis showing predicted model outputs as the indicated parameter (K_S, K_{O_2}, $K_{initial}$, or Flow Rate) was altered from –50 to +100% of its default value. (a) Maximum biomass concentration. (b) Maximum rate of substrate utilization. (c) Total percent reduction in substrate concentration during the 10-day simulation period. (d) Maximum temperature.

(fig. 5d); however, the maximum concentrations of X were significantly altered (fig. 5a). Again, the rates of degradation, temperature levels, and total substrate reduction were regulated by changes in the oxygen and temperature levels and their effects on microbial growth rates. The system of equations tended to either increase or decrease biomass growth and concentrations which resulted in remarkably similar rates of composting. Higher values of β_{max} or lower values of $Y_{X/S}$ resulted in slightly earlier (approximately 5 to 10 h) occurrences of the peak values.

Higher values of K_{O_2} or K_S tended to decrease all the response variables plotted (figs. 6a through 6d) as would be anticipated due to lower growth rates; however, the sensitivities (slopes of lines in fig. 6) to these changes were extremely small. This was primarily due to the relatively high levels of substrate in the mixture and the relatively high air flow rate which maintained generally adequate oxygen levels. Again, the changes in X_{max} (6.8% for K_S and 5.3% for K_{O_2}) were higher than the changes in the other outputs due to the self-regulating nature of the process.

Changes in the initial biomass concentrations (X_{init}) had extremely small effects (figs. 6a through 6d) on the magnitudes of the output values examined (less than 0.2%); however, the times at which the maximum values were achieved shifted. For example, the maximum rate of substrate degradation occurred at 189 h for X_{init} = 0.004 kg/m^3 and at 165 h for X_{init} = 0.016 kg/m^3.

Changing the aeration rate (F; $kg_{da} \cdot h^{-1} \cdot m^{-3}$) from 5 to 20 resulted in major changes in all output variables except maximum temperature which only decreased from 69.7°C at F = 5 $kg_{da} \cdot h^{-1} \cdot m^{-3}$ to 68.1°C at F = 20 $kg_{da} \cdot h^{-1} \cdot m^{-3}$ (figs. 6a through 6d). The effect of airflow rate on the composting process is shown in more detail in figures 2a through 2f. Higher air flow rates provided more optimal conditions (figs. 2d through 2e) during the time periods when rapid composting was occurring, but they also caused more rapid moisture depletion (fig. 2f). This moisture depletion caused the durations of these higher rates to be shorter and the total substrate degradation was lower at 15 and 20 $kg_{da} \cdot h^{-1} \cdot m^{-3}$ than at 10 $kg_{da} \cdot h^{-1} \cdot m^{-3}$ (figs. 2c and 6c).

Laboratory Results

Figures 7a and b present results from the laboratory composting trial. Oxygen uptake rate and compost temperatures as a function of time are shown for the composting mixture used in this study. Total weight loss from the composter during the 10-day trial was approximately 36%. Total dry matter loss was approximately 26%. Significant volume reduction was noticeable, with the depth decreasing by 20% and with a shrinkage in compost diameter away from the walls in the top half of the composter. The space between the compost mass and the walls was approximately 3 cm at the top surface. Significant consolidation and packing occurred within the center of the composter and probably resulted in nonuniform air flow through the compost mass. A definite moisture difference existed between the top (approximately 31%) and the bottom (approximately 68%). With the exception of the top layer, in which the thermocouple probe

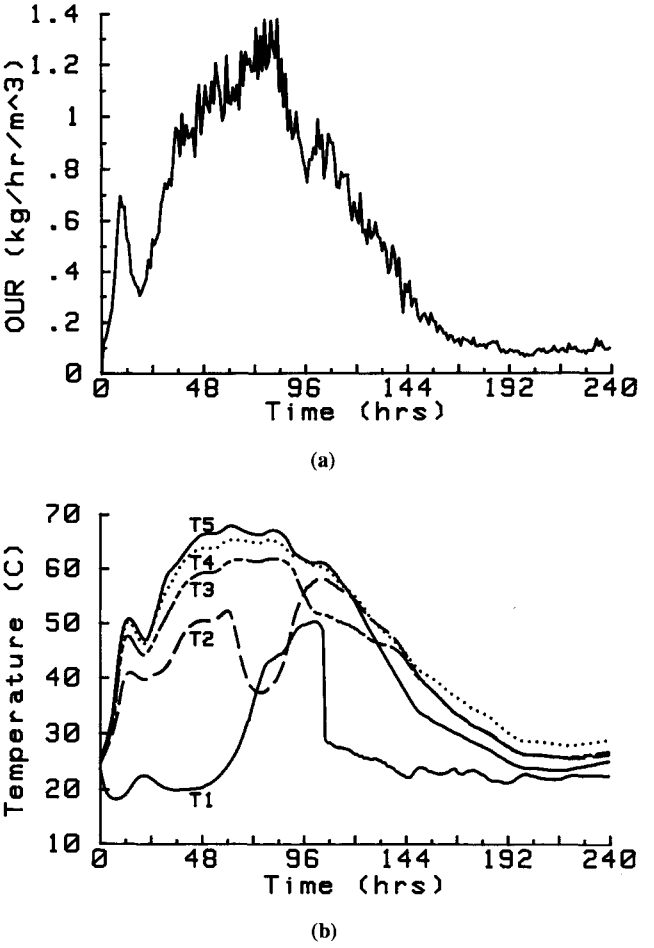

Figure 7–Experimental results from laboratory composter with a constant aeration rate of 15 $kg_{da}/(h \cdot m^3)$. (a) Oxygen uptake rate [OUR, $kg/(h \cdot m^3)$]vs. time. (b) Temperature in each layer vs. time [inlet at T1 (top), exhaust from T5 (bottom)].

was above the compost mass at the end of the trial, the thermocouple probes were bent and tended to follow the compost levels down as the volume decreased.

The maximum oxygen uptake rate of approximately 1.25 $kg_{O_2} \cdot h^{-1} \cdot m^{-3}$ (fig. 7a) corresponds to a maximum substrate degradation rate of 0.9 $kg \cdot h^{-1} \cdot m^{-3}$. The experimental composter was operated with a flow rate of 15 $kg_{da} \cdot h^{-1} \cdot m^{-3}$ for which the predicted maximum rate of substrate degradation was 0.75 $kg \cdot h^{-1} \cdot m^{-3}$ (figs. 2b and 6b). The experimental data do not include the initial 22-h lag phase which was not monitored experimentally. The experimental temperature profiles shown in figure 7b exhibit some of the predicted patterns illustrated in figures 1d and 3d. The incremental increases in temperatures between each successive layer reflected the microbial activity and substrate degradation occurring within that layer and were consistent with the shifting patterns of biomass activity predicted by the model. The delayed increase and the rapid decrease in temperature observed for the first layer was predicted reasonably well. The most rapid phase of the experimental decrease probably occurred when the thermocouple probe in the top layer became exposed to the inlet air stream at approximately 108 h (fig. 7b).

The rapid increase in temperature followed by a brief decline was very pronounced in the experimental data. This was not predicted by the model for cases with constant air flow (fig. 1d). Figure 2b does illustrate some small predicted oscillations in the rate of substrate degradation caused by the effect of temperature on μ_{max} and β_{max}. Other oscillations (again caused primarily by the effect of temperature on μ_{max}) are evident in figures 1a, 1b, and 1e, but only small temperature oscillations were predicted (fig. 1d). Other authors (Haug, 1980) have observed similar oscillations and have attributed the oscillations to shifts in growth rates as thermophilic bacteria replace mesophilic bacteria. This could be modeled more completely by slight modifications in the ktemp term if additional substantiating information was available.

SUMMARY

The model, as currently formulated, provides an excellent vehicle for explaining and demonstrating the complex interactions which occur in the composting process. As such, it also provides an excellent tool for students to evaluate design alternatives (Stombaugh and Nokes, 1994). The model appears to provide realistic predictions of temperature fluctuations, oxygen uptake rate, moisture exchanges, and substrate degradation for a readily composted input mixture. The model also provides a fundamental analysis which can be further evaluated and developed to provide a biologically based treatment of this complex process. Complete verification of the model will require substantially more data on the growth and maintenance of biomass (microorganisms) during the composting process.

Little data are available to either confirm or reject the predicted biomass levels. The predicted levels appear to be relatively high, but these predicted levels could be modified with relatively little effort as better information becomes available. For example, increasing k_d and β_{max} slightly and decreasing $Y_{X/S}$ slightly would result in lower predicted values of biomass (fig. 5a) without substantial changes in other predicted outputs (figs. 5b-d). The parameter values currently used for μ_{max}, β_{max}, $Y_{X/S}$, and k_d have been selected to provide realistic outputs while remaining consistent with coefficient values used in biochemical process engineering and wastewater treatment texts. As growth and death rates as well as yield coefficients are refined, the formation of biomass from substrate and the return of biomass to substrate could be included in the stoichiometric equations and in the differential equations for biomass (eq. 1) and substrate (eq. 2).

If this model is to be adapted to research purposes, it may be desirable to incorporate several additional refinements. Anticipated alterations could account for the effects of C/N ratio and the effects of moisture content, particle size, and substrate solubility on biomass growth. The effects of C/N ratio could be included by separating the substrate term in equations 2, 3, and 4 into energy and protein components. This technique has been successfully used to predict swine growth as a function of energy and protein intake (Stombaugh and Stombaugh, 1991). To describe the effects of moisture content, particle size (surface area), and substrate solubility on biomass growth, the substrate concentrations and half-velocity constants in equations 3 and 4 could be quantified using solubility, diffusion, and mass transfer concepts (Bailey and Ollis, 1986; Hamelers, 1993; Shuler and Kargi, 1992). In addition, this model has assumed no changes in volume with respect to time. Although this would further complicate the analysis, volumetric changes could be included.

ACKNOWLEDGMENTS. The authors thank the students in the 1992, 1993, and 1994 classes of A.E. 625 who contributed to the development of this project. Special thanks are due Mr. K. C. Das who initially proposed applying bioprocess modeling techniques to composting and Mr. Rugang Qi who completed a thorough analysis and evaluation of a previous version of the model. We would also like to thank Charles and Eugene Sukup of the Sukup Manufacturing Company for providing cost data and for discussing mixing and handling alternatives. The authors are also grateful to Dr. H. M. Keener for helpful descriptions and discussions of the composting process.

REFERENCES

Bailey, J. E. and D. F. Ollis. 1986. *Biochemical Engineering Fundamentals,* 2nd Ed., 984. New York: McGraw-Hill.

Boeckh, E. H. 1994. *Agricultural Building Cost Guide,* 84. New Berlin, Wis.: Thomson Publishing Corp.

Elwell, D. L., H. M. Keener, H. A. J. Hoitink, R. C. Hansen and J. Hoff. 1994. Pilot and full scale evaluations of leaves as an amendment in sewage sludge composting. *Compost Sci. and Utilization* 2(2):55-74.

Hamelers, H. V. M. 1993. A theoretical model of composting kinetics. In *Science and Engineering of Composting: Design, Environmental, Microbiological and Utilization Aspects,* 36-58, eds. H. A. J. Hoitink and H. M. Keener. Worthington, Ohio: Renaissance Publications.

Hansen, R. C., H. M. Keener, C. Marugg, W. A. Dick and H. A. J. Hoitink. 1993. Composting of poultry manure. In *Science and Engineering of Composting: Design, Environmental, Microbiological and Utilization Aspects,* 131-153, eds. H. A. J. Hoitink and H. M. Keener. Worthington, Ohio: Renaissance Publications.

Haug, R. T. 1980. *Compost Engineering, Principles and Practices,* 655. Lancaster, Pa.: Technomic Publishing Co., Inc.

————. 1986a. Composting process design criteria. Part I – Feed conditioning. *BioCycle* August:38-43.

————. 1986b. Composting process design criteria. Part II – Detention Time. *BioCycle* September:36-39.

————. 1986c. Composting process design criteria. Part III – Aeration. *BioCycle* October:53-57.

Haug, R. T. and L. D. Tortorici. 1986. Composting process design criteria. Part IV – Case study. *BioCycle* November/ December:34-39.

Higgins, A. J., S. Chen and M. E. Singley. 1982. Airflow resistance in sewage sludge composting aeration systems. *Transactions of the ASAE* 25(4):1010-1014, 1018.

Hogan, J. A., F. C. Miller and M. S. Finstein. 1989. Physical modeling of the composting ecosystem. *Applied and Environmental Microbiol.* 55(5):1082-1092.

Keener, H. M., H. A. J. Hoitink, C. Marugg and R. C. Hansen. 1991. Design parameters for in-vessel poultry manure composting. ASAE Paper No. 91-4001. St. Joseph, Mich.: ASAE.

Keener, H. M., R. C. Hansen and D. L. Elwell. 1993a. Pressure drop through compost: Implications for design. ASAE Paper No. 93-4032. St. Joseph, Mich.: ASAE.

Keener, H. M., C. Marugg, R. C. Hansen and H. A. J. Hoitink. 1993b. Optimizing the efficiency of the composting process. In *Science and Engineering of Composting: Design, Environmental, Microbiological and Utilization Aspects*, 59-94, eds. H. A. J. Hoitink and H. M. Keener. Worthington, Ohio: Renaissance Publications.

Person, H. L. and W. H. Shayya. 1994. Composting process design computer model. *Applied Engineering in Agriculture* 10(2):277-283.

Shuler, M. L. and F. Kargi. 1992. *Bioprocess Engineering: Basic Concepts*, 479. Englewood Cliffs, N.J.: Prentice-Hall, Inc.

Stombaugh, D. P. and I. A. Stombaugh. 1991. Modeling protein synthesis and deposition during swine growth. *Transactions of the ASAE* 34(6):2522-2532.

Stombaugh, D. P. and S. E. Nokes. 1994. Aerobic composting simulation in a bioprocess engineering course. ASAE Paper No. 94-3616. St. Joseph, Mich.: ASAE.